JOURNAL OF MATERIALS SCIENCE 16 (1981) 2781–2788

Microplasticity at room temperature of single-crystal titanium carbide with different stoichiometry

E. BREVAL
Laboratory of Applied Physics I, Technical University of Denmark, Building 307, DK-2800 Lyngby, Denmark

Single crystals of titanium carbide with a C-to-Ti range of 0.64 to 0.99 were plastically deformed at room temperature with a hardness indenter and a drill. The operating slip systems were determined by hardness anisotropy and transmission electron microscopy. The results were characteristic for bulk material deformation of TiC, below, as well as above, the brittle-to-ductile transition temperature. A typical low temperature behaviour is the formation of cracks and dislocation motion along the slip systems $\{1\,1\,0\}\langle 1\,1\,0\rangle$ and $\{1\,0\,0\}\langle 1\,1\,0\rangle$, which are both common in the rock-salt structure. The high temperature deformation is characterized by the slip system $\{1\,1\,1\}\langle 1\,1\,0\rangle$. The degree of plastic deformation and the importance of the slip system $\{1\,1\,1\}\langle 1\,1\,0\rangle$ increases as the C-to-Ti ratio decreases from 0.99 to 0.64.

1. Introduction

TiC belongs to the class of the technically important so-called "interstitial" compounds of transition metals consisting of large metal atoms with small carbon atoms in the spaces between. The family of Group IV and Group V monocarbides, to which TiC belongs, possesses the rock-salt structure. The large Ti atoms form an fcc lattice interpenetrated by another fcc lattice of the small carbon atoms. Though the structure is typical for ionic materials the bond is predominantly of covalent nature. Electron charge is transferred from the carbon 2p electrons to the strong covalent metal–metal π bonds resulting in a high Peierls stress. This means that any movement of dislocations is restricted by lattice resistance [1, 2]. The strong covalent bond is responsible for the brittle behaviour of TiC. The fracture is either conchoidal or a pronounced crystallographic cleavage mainly along $\{1\,0\,0\}$ [1–3]. In spite of the brittleness, microplasticity has been found in localized regions around hardness indentations revealed by slip lines. The slip system $\{1\,1\,0\}\langle 1\,1\,0\rangle$ has been found at temperatures below 600 to 800° C [2–6]; it has only two independent slip combinations, while $\{1\,1\,1\}\langle 1\,1\,0\rangle$, which dominates above 600 to 800° C, has five independent slip combinations which is enough for continuous plastic deformation of a polycrystalline material [2, 5, 6]. At high temperatures the electronic state changes. The concentration of conduction electrons is increased and the metallic bond prevails. The resemblance to an fcc metal is pronounced and the metallic character of TiC predominates. The rock-salt structure of TiC indicates that a $\{1\,0\,0\}\langle 1\,1\,1\rangle$ slip may possibly also exist [7].

The cubic monocarbides are characterized by stable non-stoichiometric phases. In TiC_x, x ranges from approximately 0.5 to 1. Many properties are dependent on the C-to-Ti ratio. The critical resolved shear stress, and hence the hardness, decreases with decreasing x [2–5]. The same deformation mechanism is operating in TiC_x as in the stoichiometric TiC, only the $\{1\,1\,1\}\langle 1\,1\,0\rangle$ is a little more pronounced at lower temperatures [5]. The study of the nucleation and motion of dislocations with microhardness measurements and electron or optical microscopy has been intense [1–6, 8, 9]. Electron microscope observations of

0022–2461/81/102781–08$02.80/0

dislocations in TiC deformed at elevated temperatures have been reported [6, 8]. Earlier investigations [3, 9] showed evidence of at least one slip system, $\{1\,1\,1\}\langle 1\,1\,0\rangle$, in TiC deformed at room temperature. The present paper describes microplasticity at room temperature in single-crystal TiC with a different C-to-Ti ratio. The operating slip systems were determined from anisotropy in hardness and from transmission electron microscope (TEM) observations of specimens deformed by hardness indentations and drilling.

2. Experimental procedures

The samples were obtained from three types of crystals grown by the floating-zone technique having C-to-Ti ratios of 0.99, 0.79 and 0.64. The crystallographic orientation of pieces of the crystal was easily found by the help of the distinct $\{1\,0\,0\}$ cleavage. Blocks of approximately 3 mm × 5 mm × 8 mm were either cut or made by cleavage, the large face being an $\{1\,0\,0\}$ cleavage face. The specimens were then ground and polished after moulding in an epoxy matrix. Vickers hardness measurements were performed at room temperature on the polished surface. Other cleaved pieces of approximate size 3 mm × 5 mm × 5 mm were moulded into an epoxy matrix and cut into slices of thickness 0.2 to 0.3 mm. They were ground to discs with a diameter of 3 mm in order to fit the specimen holder in the electron microscope. The normal to the discs was either $\langle 1\,0\,0\rangle$, $\langle 1\,1\,0\rangle$ or $\langle 1\,1\,1\rangle$. From each of the three TiC compositions (C/Ti 0.99, 0.79 and 0.64) 45 to 50 specimens were made. One third of these were deformed by hardness indentations, one third by drilling while the remaining third were kept as a reference. The deformation was carried out on both sides of the specimens in order to increase the possibility of the electron transparent foil being in a deformed part of the crystal. The hardness indentations were performed using a Vickers hardness apparatus with a load of 500 g. Approximately 200 indentations with a spacing of 20 to 25 μm were made in single or double rows along the diameters on each side of the specimen. The drilling was made with a dentist's hard metal drill (12000 rpm). A force of approximately 5 N was applied. Rows of holes, 0.2 to 0.5 mm in diameter and up to 0.1 mm deep were made during 5 to 30 sec. The discs were thinned with a double-jet technique using an electrolyte of perchloric acid, butanol and methanol in the ratio 1:4:10 by volume. The specimens were thinned at a temperature of -15 to -20° C with a current density of 15 mA mm^{-2} and were examined in a JEOL 200 kV transmission electron microscope.

3. Results

The hardness of the three TiC compositions is presented in Fig. 1 which shows clearly a decreased hardness with decreased C-to-Ti ratio. In all the specimens anisotropy is present: minima appear at angles of 0°, 45° and 90° between $\langle 1\,0\,0\rangle$ on a $\{1\,0\,0\}$ plane and one diagonal of the diamond indenter. The anisotropy decreases with decreased stoichiometry. Each point represents the average of five readings and the standard deviations are also indicated.

In order to separate the possible slip systems, $\{1\,0\,0\}\langle 1\,1\,0\rangle$, $\{1\,1\,0\}\langle 1\,1\,0\rangle$ and $\{1\,1\,1\}\langle 1\,1\,0\rangle$, with transmission electron microscopy, a diagram was constructed (Fig. 2) showing projections of the slip planes $\{1\,0\,0\}$, $\{1\,1\,0\}$ and $\{1\,1\,1\}$ in crystals with foil normals (coinciding with the electron beam) $\langle 1\,0\,0\rangle$, $\langle 1\,1\,0\rangle$ and $\langle 1\,1\,1\rangle$. The slip direction is indicated with lines which in fact coincide with possible screw dislocations. This diagram was used for identification of slip systems during the electron microscopy procedure. If the foil normal was not precisely along the $\langle h\,k\,l\rangle$ direction trace analysis was often necessary. Fig. 2 shows that the easiest and most unambiguous identification of slip systems could be made in the $\{1\,0\,0\}$ foil because small misorientations (up to 10°) could not lead to mistakes. Besides, the determination of slip planes would not be confused by dislocations with both screw and edge character.

In the undeformed TiC specimens only a few isolated dislocations and occasionally a low angle grain boundary were observed. In the deformed specimens the number of dislocations was significantly increased and all three mentioned slip systems were observed for all three TiC compositions. Etch pits from the polishing could be found in the thin foil. They could often be distinguished from pits formed from hardness indentations and drilling holes which were found in regular rows. Often activated slip planes passed areas near hardness indentations and close to holes from the drilling.

One example of a $\{1\,0\,0\}$ slip is shown in Fig. 3. A row of dislocations with $\langle 1\,1\,0\rangle$ direction is lying in a $\{1\,0\,0\}$ plane almost perpendicular to the foil.

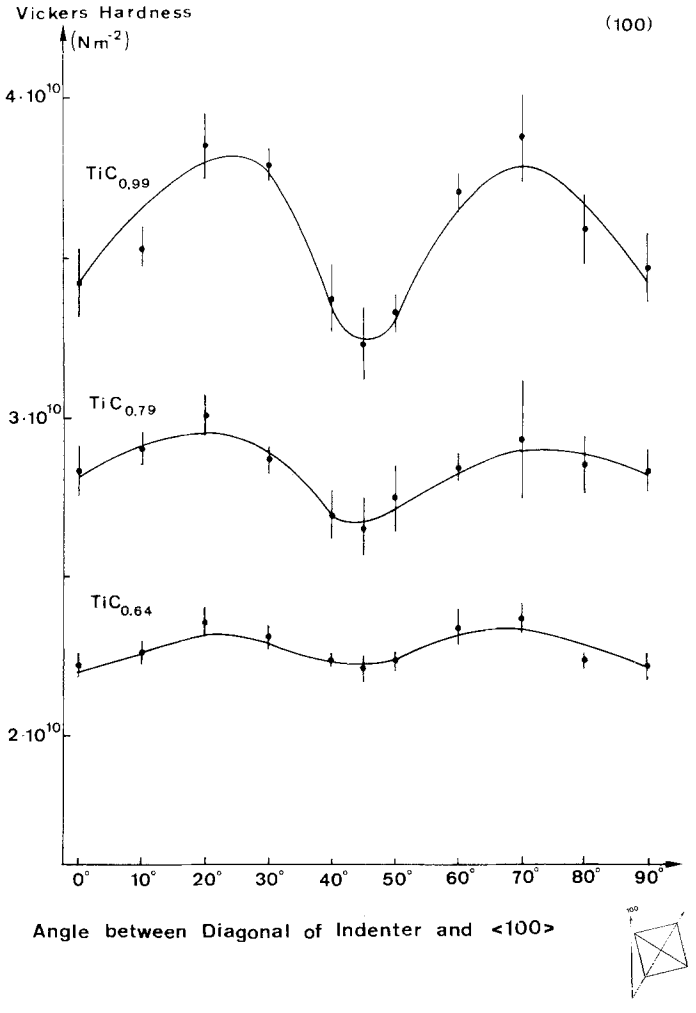

Figure 1 Hardness in single-crystal TiC. The minimum at 45° indicates that the slip system $\{1\,1\,0\}\langle 1\,1\,0\rangle$ is active. The minima at 0° and 90° indicate that $\{1\,1\,1\}\langle 1\,1\,0\rangle$ or $\{1\,0\,0\}\langle 1\,1\,0\rangle$ or both systems are operating.

The dislocation marked A possibly lies in the same plane but belongs to another dislocation family. A typical edge-on observation of a $\{1\,1\,0\}$ slip plane is presented in Fig. 4. The single dislocations are not lying parallel to the foil surface, which means that the dislocations on this $\{1\,1\,0\}$ slip plane have a partly edge character. This observation is supported by the arrangement of the dislocations in Fig. 5 which are mixed and lie in the $\{1\,1\,0\}$ plane. A typical example of $\{1\,1\,1\}\langle 1\,1\,0\rangle$ slip systems is seen in Fig. 6. A network of dislocations passes through an etch pit where a drilled hole has been. The dislocations are found to lie in two $\{1\,1\,1\}$ slip planes. As the foil normal is $\langle 1\,0\,0\rangle$, direct comparison with Fig. 2 is possible. Another network of dislocations is recorded in Fig. 7. Near the pit H, probably formed at a hardness indentation, slip has occurred. The dislocations in this network are marked DEF on the micrograph. Fig. 2 tells that the network probably lies on a $\{1\,1\,1\}$ plane as the foil normal is $\langle 1\,0\,0\rangle$. Further out from the indentation three families of dislocations A, B and C are found in another network. The slip plane cannot be unambiguously determined but it is seen from Fig. 2 that $\{1\,0\,0\}$ or $\{1\,1\,0\}$ or both of them are possible. An example of the observation of different slip planes is shown in Fig. 8 with an edge-on observation of a similar network which is possibly located in $\{1\,0\,0\}$ and $\{1\,1\,0\}$. Yet another combination of two different slip planes is seen in Fig. 9: $\{1\,1\,1\}$ slip and $\{1\,0\,0\}$ slip are observed together with a $\{1\,0\,0\}$ cleavage. An interesting deformation feature is observed at the end of some of the $\{1\,0\,0\}$ cleavage cracks (Fig. 10). A complicated tangle of dislocations is found mainly along a $\{1\,0\,0\}$ slip band near the tip of the crack. It was not possible to determine the Burgers vector because of the heavy distortion of the TiC lattice around the dislocations and the small size of the network.

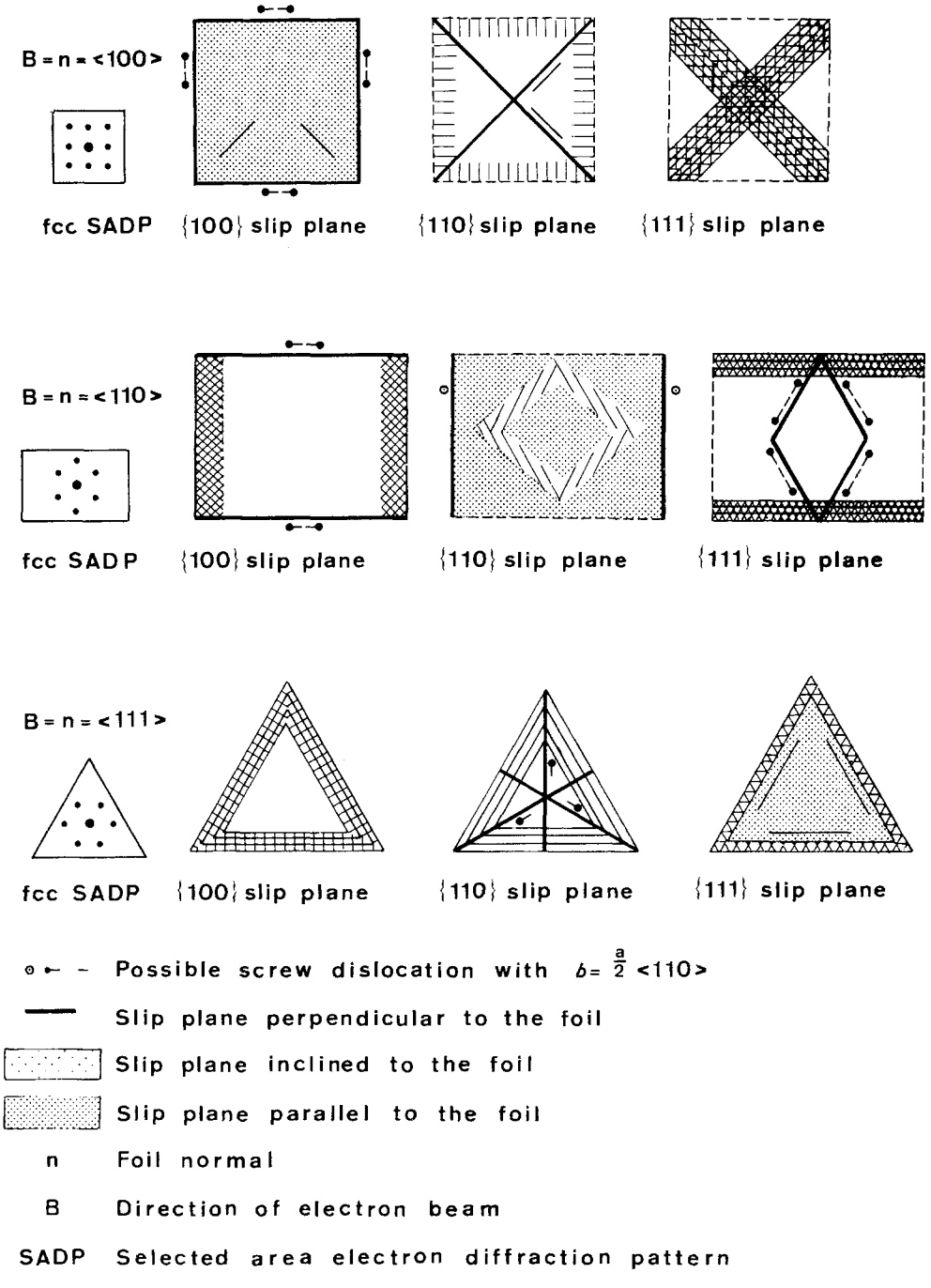

Figure 2 Diagram for identification of slip systems in cubic materials. The figure indicates possible projections of slip planes and slip directions as seen through different $\{h\,k\,l\}$ foils.

The above mentioned slip systems, cracks and dislocations associated with cracks have been observed in all the deformed TiC specimens but there was a tendency to fewer cracks with a decreased C-to-Ti ratio It was not possible to carry out a quantitative determination of the degree of plastic deformation as a function of stoichiometry by transmission electron microscopy.

4. Discussion

The hardness anisotropy phenomenon in cubic carbides is explained by the magnitude of the critical resolved shear stress for the slip systems in

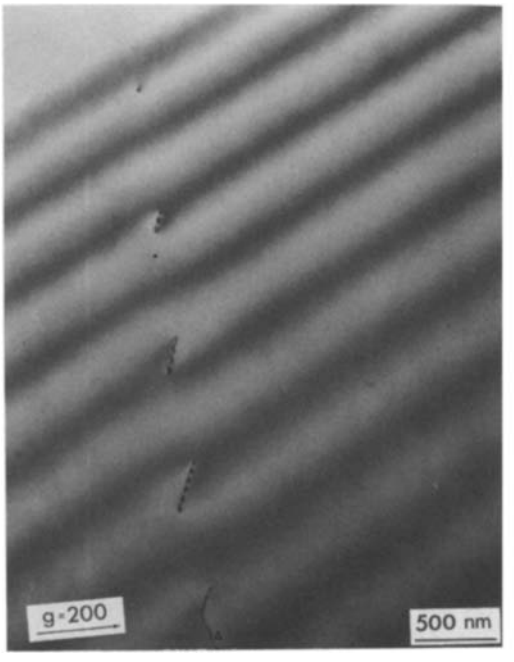

Figure 3 Bright-field TEM of the slip system $\{1\,0\,0\}\langle 1\,1\,0\rangle$. The foil normal is near $\langle 1\,0\,0\rangle$. A row of dislocations in a $\{1\,0\,0\}$ plane is observed. The specimen is $TiC_{0.99}$ deformed with a Vickers diamond.

Figure 5 Bright-field TEM of the $\{1\,1\,0\}\langle 1\,1\,0\rangle$ slip system together with another slip system, possibly $\{1\,1\,1\}\langle 1\,1\,0\rangle$. The dislocations have a mixed screw/edge character. The specimen is $TiC_{0.79}$ deformed with a Vickers diamond. The foil normal is $\langle 1\,0\,0\rangle$.

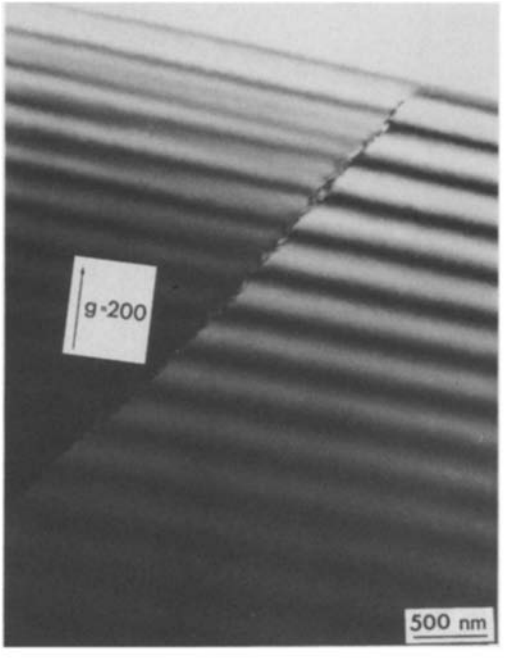

Figure 4 Bright-field TEM of the slip system $\{1\,1\,0\}\langle 1\,1\,0\rangle$. The foil normal is $\langle 1\,0\,0\rangle$. The dislocations have a partly edge character. They lie in a $\{1\,1\,0\}$ plane which is perpendicular to the foil. The specimen is $TiC_{0.64}$ deformed with a dentist's drill.

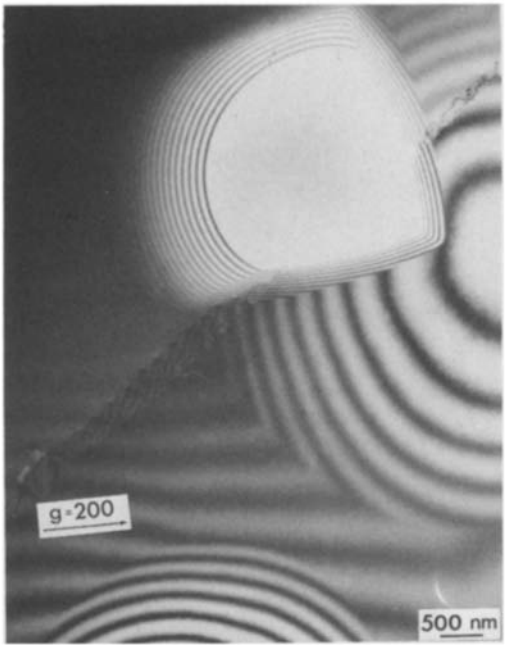

Figure 6 Bright-field TEM of an example of $\{1\,1\,1\}\langle 1\,1\,0\rangle$ slip. The foil normal is $\langle 1\,0\,0\rangle$. The large etch pit originates from a drilled hole. The specimen is $TiC_{0.64}$ deformed with a dentist's drill.

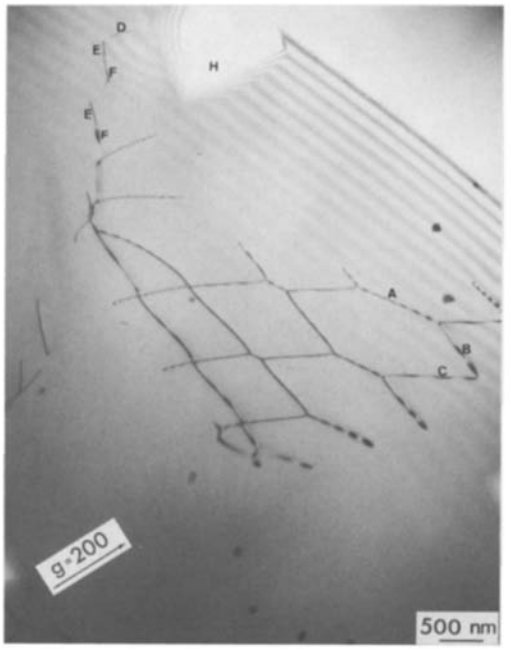

Figure 7 Bright-field TEM of an arrangement of dislocations near hardness indentation H. The network consisting of three families of dislocations (marked DEF) belongs to the slip system $\{1\,1\,1\}\langle 1\,1\,0\rangle$. The slip plane for the dislocation families A, B and C is near the foil which is $\{1\,0\,0\}$ but possibly more than one slip plane is operating. The specimen is $TiC_{0.64}$ deformed with a Vickers diamond.

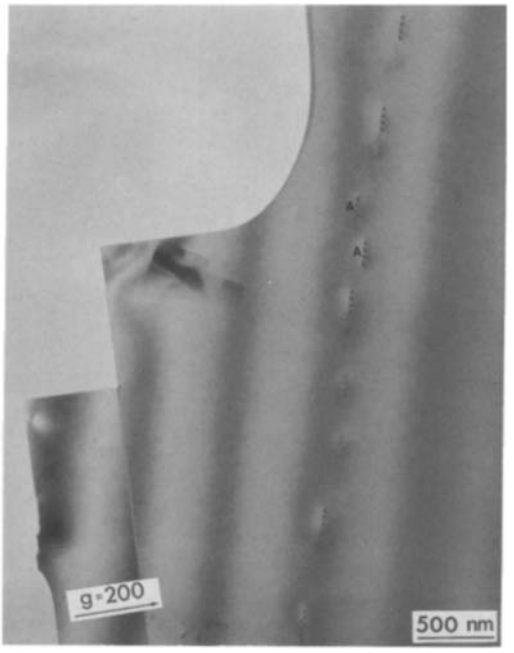

Figure 8 Bright-field TEM of an edge-on view of a network in different slip planes possibly $\{1\,0\,0\}$ and $\{1\,1\,0\}$. Note the distinct $\{1\,0\,0\}$ cleavage and the curved crack. The specimen is $TiC_{0.79}$ deformed with a Vickers diamond.

question: $\{1\,0\,0\}\langle 1\,1\,0\rangle$, $\{1\,1\,0\}\langle 1\,1\,0\rangle$ and $\{1\,1\,1\}\langle 1\,1\,0\rangle$ [4]. The minimum at an angle of 45° found with the Vickers diamond is evidence for the slip system $\{1\,1\,0\}\langle 1\,1\,0\rangle$ being active. This slip system is found in many cubic carbides at comparatively low temperatures [3–5, 8, 9]. The minima at 0° and 90° indicate that $\{1\,0\,0\}\langle 1\,1\,0\rangle$ or $\{1\,1\,1\}\langle 1\,1\,0\rangle$ or both are also active. These slip systems are generally not often reported for TiC deformation at room temperature [1, 2, 4, 10]; only Rowcliffe and Hollox [5] have done so. The hardness diagram presented by Williams [1, 2] shows a tendency in the same direction. The hardness indentations in the present study were made with a Vickers diamond which means that the indentations were squares and hence the anisotropy is less pronounced than for a Knoop diamond which gives rhombic indentations [4]. The decrease of the hardness with decreased C-to-Ti ratio is well known [1, 2], so also is the anisotropy of hardness in single-crystal TiC [2, 4, 5, 8–10] but the present investigation (Fig. 1)

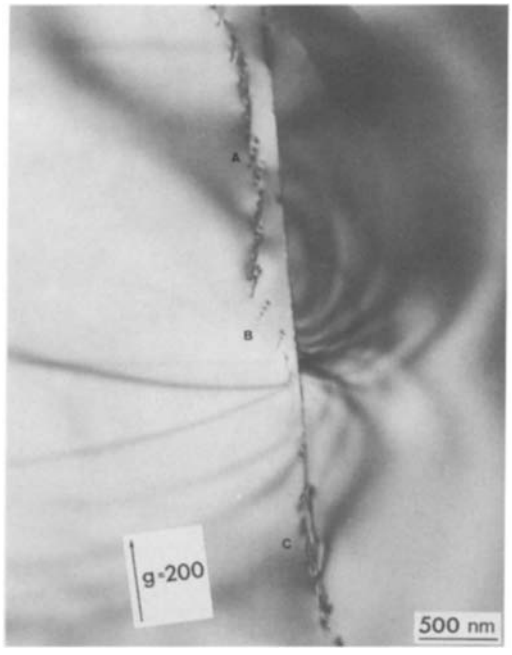

Figure 9 Bright-field TEM of a row of dislocations near a crack in $TiC_{0.79}$ deformed with a Vickers diamond. The row of dislocations belongs to $\{1\,0\,0\}\langle 1\,1\,0\rangle$ (A and C) and $\{1\,1\,1\}\langle 1\,1\,0\rangle$ (B). The foil normal is near $\langle 1\,0\,0\rangle$.

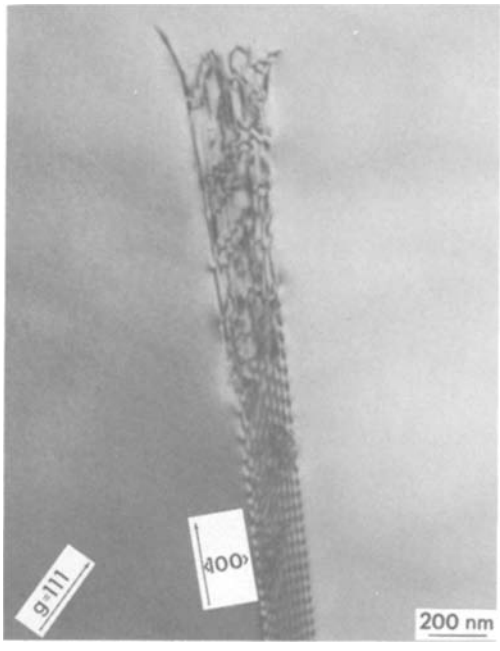

Figure 10 Bright-field TEM of a tangle of dislocations at the end of a crack along $\{1\,0\,0\}$. The specimen is $TiC_{0.79}$ deformed with a Vickers diamond. The foil normal is $\langle 1\,0\,0\rangle$.

shows the hardness to depend both on stoichiometry and on slip anisotropy.

Many of the electron microscopy observations showed that more than one slip system could operate during a localized deformation. Very often two slip systems were found giving curved rows of dislocations (Figs 5, 7, 8 and 9). It might be expected that a row of similarly oriented indentations would give a similar dislocation structure but this was not always the case. Although it was often possible to detect the same two operating slip systems from equivalent indentations, one slip system could dominate in one case while another could dominate only 20 μm from the first. Besides, the formation of cracks in connection with some of the indentations may complicate the plastic deformation (Fig. 9). These observations show that the handling of the specimen (cutting, grinding, polishing, mounting, hardness indentations, drilling and thinning) is very critical if any quantitative measurements are to be obtained from electron microscopy.

Both the hardness measurements and the transmission electron microscopy revealed more plastic deformation with decreased C-to-Ti ratio. However, all three hardness curves (Fig. 1) decrease about equally both at 0° (and 90°) and at 45°. This indicates that the relative importance of $\{1\,1\,0\}\langle 1\,1\,0\rangle$ slip is constant for different carbon contents. As carbon vacancies weaken the covalent π bond [5] and increase the concentration of conduction electrons there is reason to believe that the typical f c c metal slip system $\{1\,1\,1\}\langle 1\,1\,0\rangle$ dominates over $\{1\,0\,0\}\langle 1\,1\,0\rangle$ with decreased C-to-Ti ratio.

5. Conclusions

(1) Hardness indentations and drilling at room temperature in single-crystal TiC_x ($0.64 < x < 0.99$) give rise to microplasticity. Features are found, which for bulk material are typical below, as well as above, the brittle-to-ductile transition temperature.

(2) The characteristic low temperature behaviour is the formation of cracks, either conchoidal fracture or $\{1\,0\,0\}$ cleavage and the slip systems $\{1\,1\,0\}\langle 1\,1\,0\rangle$ and $\{1\,0\,0\}\langle 1\,1\,0\rangle$, both of which are common in materials with rock-salt structure.

(3) The observed typical high temperature behaviour is the operation of the slip system $\{1\,1\,1\}\langle 1\,1\,0\rangle$ which is characteristic for an f c c metal.

(4) A decrease in C-to-Ti ratio leads to an increase in plastic deformation and intensified importance of the slip system $\{1\,1\,1\}\langle 1\,1\,0\rangle$.

Acknowledgements

The author would like to thank A. Nørlund Christensen, Department of Inorganic Chemistry, University of Aarhus, for providing the crystals used. Thanks are due also to A. Thölén and A. Horsewell for useful discussions throughout the work.

References

1. W. S. WILLIAMS, *J. Appl. Phys.* **35** (1964) 1329.
2. W. S. WILLIAMS, "Progress in Solid State Chemistry V6, 3. Transition-metal Carbides" (Pergamon Press, Oxford, 1971).
3. E. BREVAL, *Scand. J. Metall.* **10** (1981) 51.
4. R. H. J. HANNINK, D. L. KOHLSTEDT and M. J. MURRAY, *Proc. Roy. Soc. London* **A326** (1972) 409.
5. D. J. ROWCLIFFE and G. E. HOLLOX, *J. Mater. Sci.* **6** (1971) 1270.
6. D. K. CHATTERJEE, M. G. MENDIRATTA and H. A. LIPSITT, *ibid.* **14** (1979) 2151.
7. J. P. HIRTH and J. LOTHE, "Theory of Dislocations", (McGraw-Hill, New York, 1968).
8. G. E. HOLLOX, *Mater. Sci. Eng.* **3** (1968/69) 121.

9. E. BREVAL, Proceedings of the 7th European Congress on Electron Microscopy, The Hague, The Netherlands, Vol. 1 (Seventh European Congress on Electron Microscopy Foundation, The Hague, 1980) p. 412.
10. Y. KUMASHIRO, A. ITOI, T. KINOSHITA and M. SOBAJIMA, *J. Mater. Sci.* **12** (1977) 595.

Received 27 January and accepted 26 March 1981.